



OPEN

Evaluation of macro- and meso-mechanical properties of concrete under the aggressiveness of landfill leachate

Wei Feng

Current researches on the mechanical properties of concrete are mainly concentrated on the aggressiveness of sulfate, chloride ion, acid and freeze–thaw cycles. However, the evolution of concrete mechanical properties aggressived by landfill leachate remains to be revealed. As the micro-nano indentation test is a new method to measure the fine/micro mechanical behavior of materials, it is used in this research to evaluate the micro-mechanics of the landfill leachate of the concrete sample surface and different aggressived depths. In addition, the evolution of the macro-mechanical properties of concrete aggressived by the landfill leachate was studied through uniaxial compression tests. The results show that the hydration products with high elastic modulus are consumed by the aggressiveness of landfill leachate, which results in a large number of microscopic cracks on the surface of the concrete. Moreover, the longer the aggressive time, the shallower the aggressive depth, and the more severe the deterioration of the micromechanical properties of the sample surface. It is also notable that the uniaxial compressive strength of the concrete samples aggressived by landfill leachate showed a linear increase and then gradually decrease. Comparing with the sodium chloride and sodium sulfate solutions, the landfill leachate has the most significant weakening effect on the elastic modulus of concrete.

Generally, the mechanical properties of concrete behave a positive correlation with the strength of its anti-aggressived ability. The better the mechanical properties, the stronger the ability of resisting aggressive ions, and the harder the internal structure to be destroyed^{1,2}. So far, very few researches have been concentrated on the mechanical properties of concrete after being aggressived by the landfill leachate, and most researches have been focused on the study of the mechanical properties of concrete aggressived by the sulfate^{3–6}, chloride ion^{7,8} and freeze–thaw cycles^{9,10}. However, researches on the evolving of the mechanical properties of concrete aggressived by landfill leachate remains to be done.

Generally, concrete aggressiveness is a process evolves from surface to inside, which can be divided into aggressived area and non-aggressived area. Since aggressived depth is one of the important parameters to distinguish the aggressived and non-aggressived areas, and traditional methods measuring concrete aggressived depth includes chemical analysis, ultrasonic detection and strength degradation, which have a certain degree of deficiencies. For example, the chemical analysis method has high accuracy, but it is not suitable for the detection of a variety of aggressive ions¹¹. Even though the ultrasonic detection method has poor accuracy, it is suitable for determining sample with large aggressived depth^{12,13}. And the strength degradation method assumes that the aggressived area does not bear force, which is inevitably inconsistent with its actual features.

Past researches took the aggressived and unaggressived area of concrete as a whole to evaluate its mechanical properties, and then determine the degree of deterioration and establish the constitutive relationship of the aggressived concrete^{14,15}. Actually, the mechanical properties at different aggressived depths are different, and the test results are greatly affected by the sample size and degree of aggressiveness. Therefore, it is necessary to study the mechanical properties of concrete at different aggressived depths.

Institute of Architecture and Civil Engineering, Yulin University, Chongwen West Road 4, Yulin 719000, China. email: wf_889@yulinu.edu.cn

Component	HLLN	NSSN	NSCN	NLLN	NLLO
Acetic acid (ml/L)	3.5	0.0	0.0	3.5	3.5
Propionic acid (ml/L)	3.5	0.0	0.0	3.5	3.5
Dipotassium hydrogen phosphate (mg/L)	15.0	0.0	0.0	15.0	15.0
Potassium bicarbonate (mg/L)	156.0	0.0	0.0	156.0	156.0
Potassium carbonate (mg/L)	162.0	0.0	0.0	162.0	162.0
Sodium chloride (mg/L)	47,588	0.0	50,000	720	720
Sodium nitrate (mg/L)	25	0	0	25	25
Sodium bicarbonate (mg/L)	1506	0	0	1506	1506
Calcium chloride (mg/L)	1441	0	0	1441	1441
Magnesium chloride hexahydrate (mg/L)	1557	0	0	1557	1557
Magnesium sulfate (mg/L)	78	0	0	78	78
Ammonium bicarbonate (mg/L)	1220	0	0	1220	1220
Ferrous sulfate (mg/L)	500	0	0	500	500
Copper sulfate pentahydrate (mg/L)	20	0	0	20	20
Manganese sulfate (mg/L)	250	0	0	250	250
Sodium sulfate (mg/L)	49,194	50,000	0	0	0

Table 1. Composition ratio of landfill leachate.

Recently, a new method of micro-nano indentation test was invented to measure the fine/micro mechanical behavior of materials, which has been widely used in the metal materials and cement-based materials¹⁶. The emerging nanoindentation technology effectively solves the defect that the traditional indentation measuring method is only suitable for larger size sample. The continuous changing of the load is controlled by the computer, and the indentation depth is measured in real time. Because of the ultra-low load characteristic, the monitoring sensor has a displacement resolution smaller than 1 nm. Therefore, it can detect a pressure depth as small as nanometers (0.1–100 nm), which is especially suitable for measuring the mechanical properties of ultra-thin materials such as thin films and coatings, as well as measuring mechanical properties of a material on the nanometer scale¹⁷.

Therefore, the micron indentation test was conducted to study the micro-mechanical properties of the concrete sample surface and different aggressived depths for different time by high-concentration landfill leachate aggressiveness group HLLN (High concentration—Landfill leachate—No osmotic pressure), landfill leachate original solution aggressiveness group NLLN (Normal concentration—Landfill leachate—No osmotic pressure), landfill leachate original solution plus osmotic pressure aggressiveness group NLLO (Normal concentration—Landfill leachate—Osmotic pressure). At the same time, the uniaxial compression test is also used to study the evolution of macro-mechanical properties of the concrete suffering aggressiveness of high-concentration landfill leachate group HLLN, sodium sulfate solution group NSSN (Normal concentration—Sodium sulfate solution—No osmotic pressure) and sodium chloride solution group NSCN (Normal concentration—Sodium chloride solution—No osmotic pressure). Moreover, related test results can be used for providing scientific basis for understanding the evolution of macro/micro mechanical properties of concrete structures under the aggressiveness of landfill leachate.

Aggressiveness tests

Test materials and aggressiveness method. Because of the limited aggressiveness rate of the landfill leachate on concrete under natural conditions, the concentration of sulfate ion and chloride ion were increased in the landfill leachate to accelerate the aggressiveness effect¹⁸. At the same time, considering the differences in aggressiveness environments, five groups including high-concentration landfill leachate aggressiveness group HLLN (High concentration—Landfill leachate—No osmotic pressure), sodium sulfate solution aggressiveness group NSSN (Normal concentration—Sodium sulfate solution—No osmotic pressure), sodium chloride solution aggressiveness group NSCN (Normal concentration—Sodium chloride solution—No osmotic pressure), landfill leachate original solution aggressiveness group NLLN (Normal concentration—Landfill leachate—No osmotic pressure), and landfill leachate original solution plus osmotic pressure aggressiveness group NLLO (Normal concentration—Landfill leachate—Osmotic pressure) were prepared. Since the contents of sulfate ion and chloride ion in the landfill leachate are relatively high¹⁸ and has greater impact on the concrete, the total concentrations of sulfate ion and chloride ion in group HLLN were increased to 50 g/L, respectively, which can accelerate the aggressiveness effect. The concentration of the remaining components was the same as that in group NLLN. In order to study the difference of aggressiveness conditions under high-concentration landfill leachate and single sodium sulfate plus sodium chloride solution, the concentrations of sulfate ion and chloride ion in group NSSN and group NSCN were set 50 g/L.

The indoor configuration of landfill leachate was used in this study to ensure the unity of the experimental variables, which can effectively avoid the influence of the composition of landfill leachate on the experimental results. The composition ratio of landfill leachate was selected according to¹⁹, and the composition ratio of each group of solutions are shown in Table 1.

Chemical compositions	SiO ₂	Al ₂ O ₃	Fe ₂ O ₃	CaO	MgO	SO ₃	K ₂ O
Cement	21.47	5.80	4.04	56.64	3.24	2.08	0.22
Fly ash	52.54	31.22	5.61	4.615	0.64	1.208	1.337

Table 2. Chemical compositions of cementitious materials (%).



Figure 1. Osmotic pressure device.

As the aggressiveness effect of the landfill leachate develops, the hydration products in the concrete reaction with the harmful substances in the landfill leachate, which inevitably influence the concrete durability. Aggressive ions such as sulfate ions and chloride ions in the landfill leachate will chemically reaction with the C–S–H gel and calcium hydroxide in the concrete hydration products, thereby causing aggressiveness to the concrete^{1–8,18,20}. In addition, the ordinary silicate cement and primary fly ash were used for the tests, and the fine aggregate was medium sand with a fineness modulus of 2.6, and the coarse aggregate was 5–25 mm continuously graded gravel. The chemical composition of cement and fly ash can be seen in Table 2. The concrete mix ratio is selected with cement:water:fly ash:fine aggregate:coarse aggregate = 1.00:0.59:0.25:2.76:3.79.

The cylindrical specimens ($\phi 150 \text{ mm} \times 150 \text{ mm}$) were cured under standard curing conditions (Temperature $20 \pm 2 \text{ }^\circ\text{C}$, humidity 95%). After the maintenance was completed, the standard cylindrical specimen of $\phi 50 \text{ mm} \times 100 \text{ mm}$ is prepared by coring, cutting and grinding. And then they were put in the high-concentration landfill leachate aggressiveness group HLLN and landfill leachate original solution aggressiveness group NSSN, respectively, so as to simulate the aggressiveness of concrete structure under different environments. Considering the underground concrete structure on the landfill site is occasionally aggressived by the flowing landfill leachate with certain pressure, the high-concentration landfill leachate aggressiveness group HLLN, sodium sulfate solution aggressiveness group NSSN, sodium chloride solution aggressiveness group NSCN, landfill leachate original solution aggressiveness group NLLN, and landfill leachate original solution plus osmotic pressure (apparatus shown in Fig. 1) aggressiveness group NLLO were prepared, among which aggressiveness groups HLLN, NSSN, NSCN, NLLN were used for conventional immersion aggressiveness without osmotic pressure, and the group NLLO was used for immersion conventional immersion aggressiveness with osmotic pressure. And test samples for the group NLLO were the cylindrical samples of $\phi 150 \text{ mm} \times 150 \text{ mm}$. In addition, a hole with a diameter of 20 mm and depth of 100 mm was drilled in the center of the cylindrical sample. As shown in Fig. 1, a high-pressure gas cylinder is used to pass nitrogen into a closed container containing waste leachate, thus providing osmotic pressure to the waste leachate. Under the osmotic pressure, the waste leachate will flow into the cylindrical hole inside the cylindrical specimen, so that the waste leachate under pressurized condition can erode from the inside to the outside of the concrete.

Micron indentation tests and principles. In order to obtain the evolution law of the meso-mechanical properties of concrete aggressived by landfill leachate, specimens aggressived by the high-concentration landfill leachate aggressiveness group HLLN, original concentration of landfill leachate aggressiveness group NLLN,

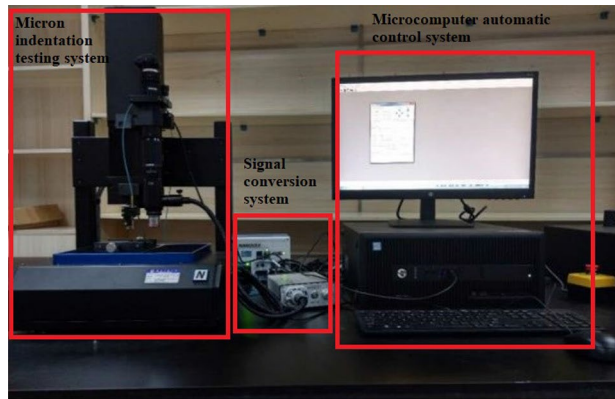


Figure 2. Micron indentation testing system.

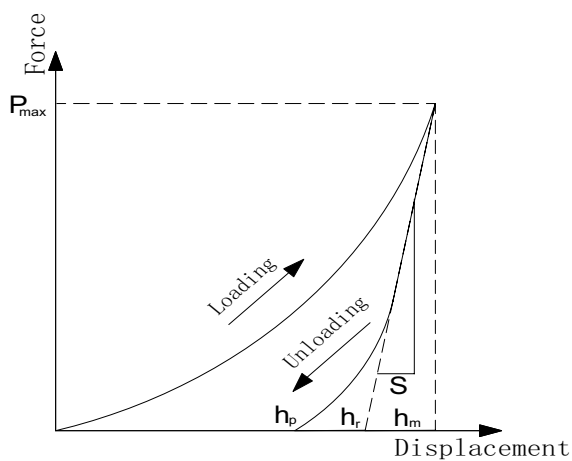


Figure 3. Loading/unloading-displacement curve.

and original solution of landfill leachate plus osmotic pressure aggressiveness group NLO were tested through micron indentation tests.

Since the concrete sample is a three-phase structure composed of hydration products, fine aggregates and coarse aggregates, and the aggressive target of the landfill leachate on the concrete is hydration products, aggressiveness on the fine aggregates and coarse aggregates are ignored in this study. According to the loading indentation tests about unaggressed specimens under different loads (5, 15, 30, and 50 N), it is concluded that no deformation damage occurred on the surface of the indentation point when the concrete suffered a maximum load of 15 N, whose indentation depth was 35 μm and indentation diameter was 0.25 mm. When the load is small (5 N), the indentation depth is shallow and generally affected by the surface roughness. However, large loads (30 N, 50 N) led to the collapse of the surface of indentation point, which eventually caused errors in the measurement results.

According to the test results and standard²¹, the maximum force of 15 N was determined in the indentation tests, and the distances from the indentation center to the boundary of the cubic sample and coarse aggregate are 2 mm, respectively. The test temperature was maintained at 24 ± 2 °C, and the micro-indentation test system is shown in Fig. 2. The distance between the centers of the two indentations are also 2 mm. In addition, a load control mode was used in the whole tests. Firstly, the sample surface was loaded linearly to 15 N with a speed of 30 N/min, and the constant load was kept constant for 10 s. Finally, samples were linearly unloaded with a speed of 30 N/min. Hence, the indentation depth curve can be obtained and the modulus of the elasticity and hardness of the hydration products can be calculated. Based on the above principles, the micron indentation tests were conducted on the cubic samples and cylindrical samples (three samples were selected in each group, each sample subjected to 30 times indentation tests).

Figure 3 shows a typical load/unload-displacement curve. The horizontal axis h is the indentation depth of the indenter, vertical axis P denotes the load, h_m means the maximum indentation depth during tests, h_p indicates the depth of the residual indentation after unloading, h_r represents the intersection between the tangent line and the horizontal axis at the maximum load of the unloading curve, and P_{max} is the maximum testing load. Based on the Oliver-Phary principle²², the elastic modulus E of a material can be calculated according the following formula:

$$\frac{1}{E_r} = \frac{1 - \nu^2}{E} + \frac{1 - \nu_i^2}{E_i} \quad (1)$$

$$E_r = \frac{\sqrt{\pi}}{2\beta} \frac{S}{\sqrt{A(h_c)}} \quad (2)$$

$$S = \left(\frac{dP}{dh} \right)_{h=h_m} \quad (3)$$

$$h_c = h_m - \varepsilon \frac{P_m}{S} \quad (4)$$

where E_r is the indentation modulus, E_i means the elastic modulus of the indenter, ν_i denotes the Poisson's ratio of the indenter. The elastic modulus and Poisson's ratio of the diamond are 1141 GPa and 0.07, respectively. ν is the Poisson's ratio of a material and generally valued 0.2–0.3 for cement-based cement hardened paste, which was valued 0.25 in this study²³. S means the contact stiffness and h_c the contacting depth between the indenter and sample. $A(h_c)$ represents the projected area of contact between the indenter and sample, which is related to the contact depth h_c . β is a constant related to the geometry of the indenter with a value of 1.012, and ε is a constant related to the shape of the indenter, which was valued 0.75.

Because of the significant difference among the concrete hydration products, the aggressiveness products of the reaction between landfill leachate and concrete are complicated, which makes the elastic moduli measured by the indentation tests are discrete. In order to obtain the distribution law of the meso-mechanical parameters of the samples, it is necessary to calculate and statistically analyze the 90 measuring points obtained from each group of experiments, so as to get the normal distribution curve and cumulative distribution curve. The normal distribution density function is

$$p(x) = \frac{1}{\sqrt{2\pi}s^2} \exp\left[-\frac{(x-\mu)^2}{2s^2}\right] \quad (5)$$

where μ is the arithmetic mean of the test value of hydration products, s means the standard deviation. μ is determined as

$$\mu = \frac{1}{N} \sum_{k=1}^N x_k, s^2 = \frac{1}{N-1} \sum_{k=1}^N (x_k - \mu)^2 \quad (6)$$

where N is the number of test data for each group, which is 90 in this study, and x_k is the elastic modulus obtained from tests.

Uniaxial compression tests. The maximum vertical force of the uniaxial compression test apparatus used in this research can reach 1000 kN and maximum confining pressure 50 MPa. In addition, both displacement controlling mode and force controlling mode can be applied in this apparatus. Therefore, the displacement controlling mode was chosen in this study. A small axial force of preloading is applied to the sample before loading, and a loading rate of 0.002 mm/s is then kept until the specimen is damaged.

Test results analysis

Micron indentation test results. Past researches revealed that the main phases of concrete hydration products are CSH gel (12.6–35.3 GPa), calcium hydroxide (33.0–44.5 GPa) and ettringite (40.0–52.0 GPa)²⁴. And the aggressive products of concrete due to the landfill leachate are ettringite and Friedel salt (whose elasticity modulus is similar to that of C-SH gel²⁵). Based on the micron indentation tests, the distribution of the elastic modulus at different aggressived depths can be obtained, and hence the distribution of different hydration products at different corrosion sites can be effectively judged.

Micron indentation test on the aggressived surface. Table 3 shows the probability distribution of the elastic modulus of the hydration products on the cubic sample surface in corroded by group HLLN for 0, 90, and 180 days, respectively. According to Eq. (5), and the probability distribution of the test results are shown Fig. 4.

Figure 4 shows that the average elastic modulus of the sample surfaces gradually decreased with aggressive time. Which also told that the average elastic modulus of hydration products was 21.55 GPa, while the average elastic modulus of hydration products on the sample surfaces decreased to 17.40 GPa and 11.23 GPa after being aggressived for 90 and 180 days, whose decrement reached 19.26% and 47.89%, respectively. Therefore, the landfill leachate has great impact on the micromechanical properties of the sample surfaces, which seriously deteriorated the micromechanical properties of the samples.

In addition, the elastic moduli of the hydration products before aggressiveness were greater than 11 GPa, most of which in the range of 27–39 GPa. It is attributed to rare pore and crack (elastic modulus in the range of 0–12.2 GPa) existed in the samples, which contained a large amount of hydration products such as C-S-H gel and calcium hydroxide with large elastic moduli (as shown in Fig. 5a). As shown in Fig. 4, with the aggressiveness continued, the distribution probability of the elastic modulus (in the range of 6–13 GPa) of the hydration

Elastic modulus interval (GPa)	Corresponding probability without aggressiveness	Corresponding probability of aggressive 90d	Corresponding probability of aggressive 180d
(6,8]	0.00	0.00	0.14
(8,10]	0.00	0.07	0.27
(10,12]	0.00	0.09	0.14
(12,14]	0.04	0.17	0.10
(14,16]	0.13	0.08	0.18
(16,18]	0.13	0.17	0.10
(18,20]	0.09	0.12	0.00
(20,22]	0.16	0.07	0.02
(22,24]	0.07	0.07	0.02
(24,26]	0.07	0.02	0.02
(26,28]	0.10	0.02	0.00
(28,30]	0.02	0.04	0.00
(30,32]	0.10	0.04	0.00
(32,34]	0.04	0.02	0.00
(34,36]	0.02	0.02	0.00
(36,38]	0.00	0.00	0.00
(38,40]	0.02	0.00	0.00

Table 3. Probability distribution of the elastic modulus after high-concentration aggressiveness.

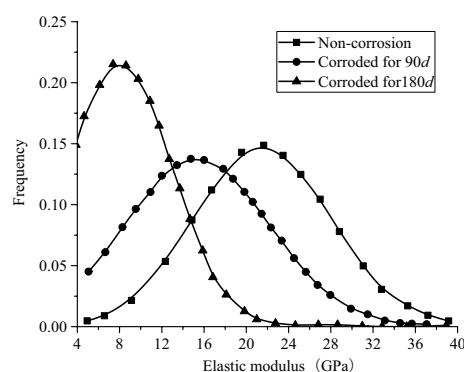


Figure 4. Probability fitting diagram of elastic modulus after high-concentration aggressiveness.

products on the sample surfaces substantially increased as they were aggressed by the high-concentration landfill leachate Group HLLN for 90 days, whose probability drastically decreased with the elastic modulus in the range of 27–39 kPa. It is attributed that with the aggressiveness continued, some microscopic cracks emerged on the surface of the sample (as shown in Fig. 5b,c), which finally led to a significant increase in the probability of the elastic modulus of the hydration products in the range of 6–13 GPa. In addition, the hydration products such as C–S–H gel and calcium hydroxide in the concrete were consumed by the landfill leachate (as shown in Fig. 5d), which led to the decrease in the distribution probability of the elastic modulus in the range of 27–39 GPa. As shown in Fig. 4, after being aggressed for 180 days, the elastic modulus of the hydration products on the surface were less than 25 GPa, which is attributed to the calcium hydroxide with high elastic modulus on the concrete surface were almost consumed by the landfill leachate, and a large number of pores, cracks, were produced. As a result, the elastic moduli in the range of 7–13 kPa of the sample surfaces were greatly increased. Therefore, the landfill leachate has great impact on the micro-mechanical properties of the concrete surfaces, which can effectively cause the overall reduction of the elastic modulus of the sample surfaces, and even lead to the deterioration of the overall micro-mechanical properties and finally result in the deterioration of the macro-mechanical properties of the samples.

Micro-indentation test at different aggressed depths. Local meso-mechanical properties at different aggressed depths aggressed by the high-concentration landfill leachate group HLLN, landfill leachate original solution group NLLN and landfill leachate original solution plus osmotic pressure group NLO for 180 days were obtained through micro-indentation tests. The probability distribution of the elastic moduli of the hydration products at corrosion depth of 0–5 mm, 5–15 mm and 15–25 mm by group HLLN and group NLLN, and the elastic modulus of hydration products at samples depth 0–2, 2–4, 5–11 and 11–16 mm corroded by group NLO

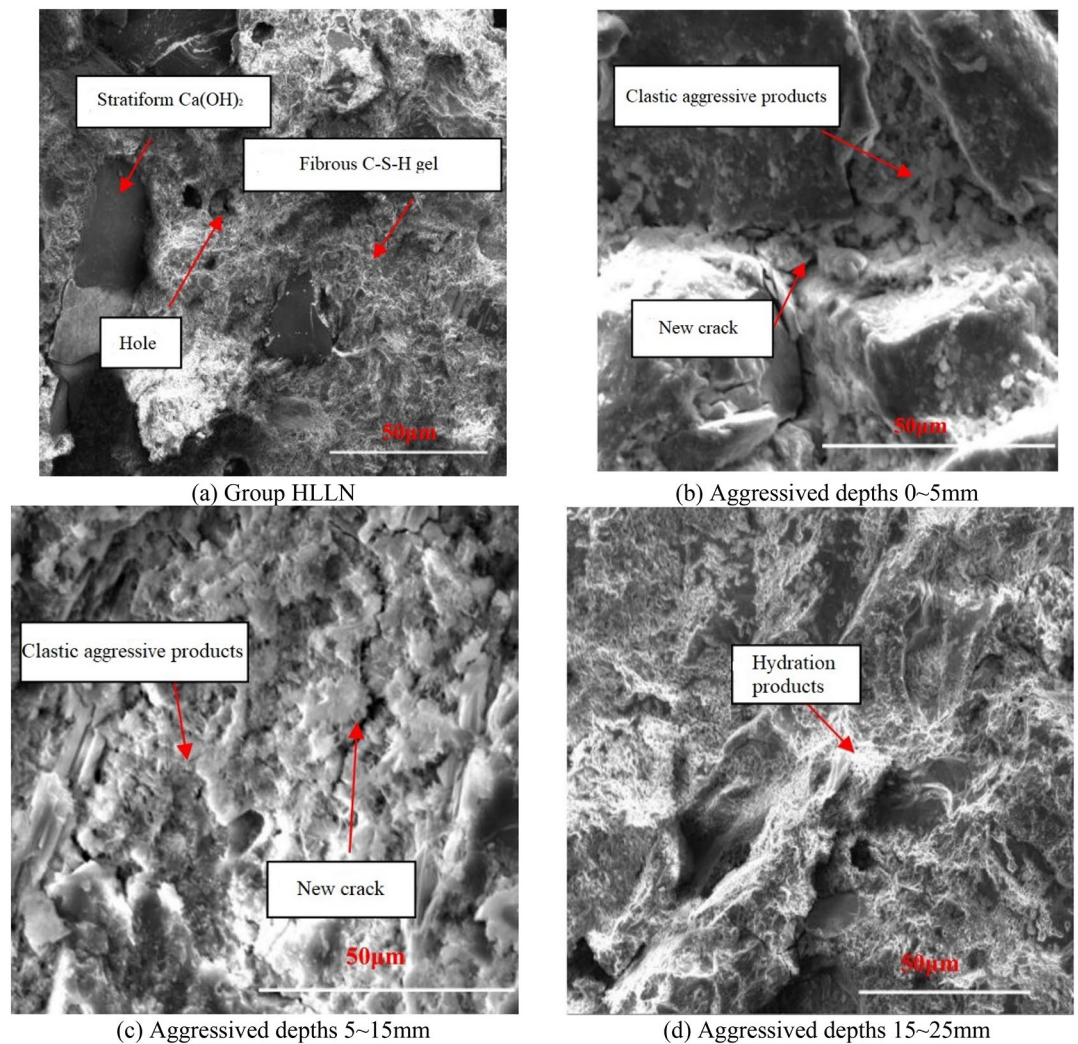


Figure 5. Scanning electron microscope of samples without erosion and after 180 days of erosion.

are shown in Tables 4, 5 and 6, respectively. In addition, the fitting results in probability distribution diagrams are shown in Fig. 6a–c).

Figure 6a shows the probability distribution of the elastic modulus of hydration products at different aggressed depths before and after aggressiveness. It is obvious that the shallower the aggressed depth, the more obvious the decrease in the average elastic modulus of the hydration products. In the innermost part of the samples, due to the continued hydration of cement and secondary hydration effect of fly ash, the meso-mechanical properties were effectively enhanced. For example, the average elastic modulus of hydration products in the aggressed depth of 0–5 mm was 19.27 GPa, whose values were 20.35 GPa and 24.46 GPa in the aggressed depths of 5–15 and 15–25 mm, respectively. At the same time, the shallower the aggressed depth, the less the content of hydration products (e.g., calcium hydroxide) with larger elastic modulus, and the more aggressed products (e.g., pores and cracks) with smaller elastic modulus. Specifically, the shallower the aggressed depth, the smaller the distribution probability of the elastic modulus of hydration products in the range of 31–39 GPa, and the greater the distribution probability of the elastic modulus in the range of 5–11 GPa. On the one hand, harmful ions such as SO_4^{2-} , Cl^- , HCO_3^- , and H^+ in the landfill leachate reaction with the hydration products (e.g., calcium hydroxide and CSH gel), a large amount of calcium hydroxide and CSH gel were consumed and eventually led to the decrease in the distribution probability of the hydration products in the range of 31–39 GPa. On the other hand, a large number of microscopic cracks (fracture elastic modulus in the range 0–12.2 GPa) generated when the sample was aggressed, which increased the distribution probability of the elastic modulus of hydration product in the range of 5–11 GPa.

As shown in Fig. 6b, the distribution probability of the elastic modulus of the hydration product aggressed by group NLLN for 180 days are the same as those in group HLLN. Which means the shallower the aggressed depth, the smaller the average elastic modulus and the smaller the probability of the elastic modulus of hydration products in the range of 31–39 GPa, and the greater the distribution probability of the elastic modulus in the range of 5–11 GPa. Nevertheless, the average elastic modulus of hydration products was slightly larger, which is due to the aggressed degree of concrete is slightly lower.

Elastic modulus interval (GPa)	Corresponding probability of aggressived depth 0–5 mm	Corresponding probability of aggressived depth 5–15 mm	Corresponding probability of aggressived depth 15–25 mm
(6,8]	0.01	0.00	0.00
(8,10]	0.03	0.01	0.01
(10,12]	0.06	0.09	0.00
(12,14]	0.02	0.04	0.01
(14,16]	0.14	0.06	0.03
(16,18]	0.12	0.14	0.12
(18,20]	0.10	0.08	0.10
(20,22]	0.18	0.11	0.14
(22,24]	0.10	0.16	0.10
(24,26]	0.08	0.07	0.03
(26,28]	0.06	0.07	0.07
(28,30]	0.04	0.06	0.07
(30,32]	0.01	0.06	0.08
(32,34]	0.01	0.04	0.06
(34,36]	0.01	0.01	0.04
(36,38]	0.01	0.01	0.07
(38,40]	0.01	0.00	0.07

Table 4. Probability distribution of the elastic modulus at different aggressived depths for group HLLN.

Elastic modulus interval (GPa)	Corresponding probability of aggressived depth 0–5 mm	Corresponding probability of aggressived depth 5–15 mm	Corresponding probability of aggressived depth 15–25 mm
(6,8]	0.00	0.00	0.00
(8,10]	0.00	0.00	0.00
(10,12]	0.04	0.02	0.00
(12,14]	0.11	0.04	0.02
(14,16]	0.07	0.10	0.06
(16,18]	0.04	0.17	0.06
(18,20]	0.11	0.08	0.10
(20,22]	0.19	0.08	0.16
(22,24]	0.30	0.20	0.10
(24,26]	0.04	0.14	0.10
(26,28]	0.11	0.04	0.16
(28,30]	0.00	0.06	0.00
(30,32]	0.00	0.02	0.10
(32,34]	0.00	0.04	0.10
(34,36]	0.00	0.00	0.00
(36,38]	0.00	0.00	0.06
(38,40]	0.00	0.00	0.00

Table 5. Probability distribution of the elastic modulus at different aggressived depths for group NLLN.

Seeing from Fig. 6c, the distribution of the elastic modulus of the hydration products is similar to those at the aggressived depths of 0–2 mm and 2–4 mm, as well as the average elastic modulus are almost the same. With the increase in aggressived depth, the average elastic modulus of hydration products significantly increased. And at aggressived depth 11–16 mm, the average elastic modulus of hydration products reached 26.51 GPa. In addition, as the aggressived depth increased, the probability of the elastic modulus of hydration products in the range of 31–39 GPa was greater, while the distribution probability of the elastic modulus in the range of 5–11 GPa was smaller, which is in consistent with the results by the group HLLN and group NLLN.

Depth of sample aggressiveness. The mechanical parameters of the surfaces and different aggressived depths can be accurately measured through micro-indentation tests. As Fig. 7 shows the relations between the mean elastic modulus of the sample surfaces and different aggressived depths versus aggressived depths without being aggressived and after being aggressived for 180 days by the high-concentration landfill leachate group HLLN, the

Elastic modulus interval (GPa)	Corresponding probability of aggressed 0–2 mm	Corresponding probability of aggressed 2–4 mm	Corresponding probability of aggressed 4–6 mm	Corresponding probability of aggressed 6–11 mm	Corresponding probability of aggressed 11–16 mm
(8,10]	0.03	0.00	0.04	0.00	0.00
(10,12]	0.00	0.06	0.00	0.03	0.00
(12,14]	0.03	0.06	0.04	0.00	0.00
(14,16]	0.03	0.06	0.04	0.03	0.00
(16,18]	0.18	0.21	0.17	0.20	0.08
(18,20]	0.10	0.06	0.12	0.08	0.00
(20,22]	0.07	0.14	0.04	0.08	0.00
(22,24]	0.21	0.03	0.08	0.00	0.24
(24,26]	0.07	0.09	0.21	0.04	0.21
(26,28]	0.10	0.09	0.00	0.16	0.04
(28,30]	0.03	0.00	0.00	0.04	0.08
(30,32]	0.08	0.06	0.04	0.11	0.04
(32,34]	0.07	0.06	0.08	0.08	0.17
(34,36]	0.00	0.03	0.08	0.08	0.00
(36,38]	0.00	0.03	0.00	0.03	0.04
(38,40]	0.00	0.00	0.04	0.03	0.04
(40,42]	0.00	0.03	0.00	0.00	0.04

Table 6. Probability distribution of the elastic modulus at different aggressed depths for group NLLO.

original landfill leachate solution group NLLN, and the original landfill leachate solution plus osmotic pressure group NLLO.

Seeing from Fig. 7, the mean elastic modulus of the specimens aggressed by the three aggressive groups for 180 days significantly increase with the increase of aggressed depth, and the internal mechanical properties of the specimens were effectively enhanced. The specimens aggressed by group HLLN behaved different in the local mechanical properties at different aggressed depths. The closer the distance to the specimen surface, the more drastic change about the mechanical properties. For example, after being aggressed for 180 days, the average elastic modulus of the hydration products on the sample surface was 11.23 GPa, while the average elastic modulus of the hydration products quickly increased to 19.27 GPa at the aggressed depth of 0–5 mm, and the mean elastic modulus of the hydration products increased slowly with aggressed depth. Which indicates that the deterioration of the surface layer of the samples are far more serious than that of the inside of samples. The evolution of the mean elastic modulus of the sample aggressed by group NLLN is similar to that of group HLLN, while the mean elastic modulus of the sample aggressed by group NLLN is slightly higher than that of group HLLN at a same aggressed depth, which indicates that the sulfate ion and chloride ion in the high-concentration landfill leachate aggressive group HLLN accelerate the aggressive process. There was no significant decreasing in the elastic modulus of the samples aggressed by group NLLO, and the mean elastic modulus of the hydration products at a depth of 0–4 mm was equal to that in the unaggressed state. In addition, the mean elastic modulus of the hydration products increased with the aggressed depth. And at the same aggressed depth, it's mean elastic modulus was greater than that of the samples aggressed by groups HLLN and NLLN. On the one hand, the osmotic pressure (0.4 MPa) applied in the test was relatively small. As a result, an effective seepage channel in the concrete did not form. On the other hand, there was a hole in the center of the sample with a diameter of 20 mm and depth of 100 mm, small osmotic pressure and dense concrete structure made it impossible for the erosive solution inside the hole to permeate and diffuse, and the aggressive speed was finally limited.

According to Fig. 8, when the samples are aggressed by group HLLN for 90 and 180 days, there are significant increase in the elastic moduli of the samples as the increase of aggressed depth, and the elastic moduli changed sharply at shallow aggressed depth and slowly increased at deep aggressed depth. In addition, when the aggressed depth is less than 14 mm, the mean elastic modulus of the samples aggressed for 90 days are greater than those aggressed for 180 days. If the aggressed depth is greater than 14 mm, the mean elastic moduli of the sample aggressed for 90 days are smaller than those aggressed for 180 days, which contributes to fact that the samples aggressed by the landfill leachate at the shallow aggressed depth behaved less deterioration on the micromechanical properties of the samples.

Uniaxial compression test results. In order to study the degradation law of the macro-mechanical properties of concrete in the landfill leachate, sodium sulfate and sodium chloride solutions, the concretes were aggressed by the high-concentration landfill leachate group HLLN, sodium sulfate solution group NSSN, and sodium chloride solution group NSCN, and the uniaxial compression test results are as follows.

Deterioration law of compressive strength. Figure 9 shows the variation of uniaxial compressive strengths of the samples after being aggressed by several solutions for a certain period of time. It is obvious that the uniaxial compressive strength can be classified into two stages: linear increase and slow decline. In the linear increase

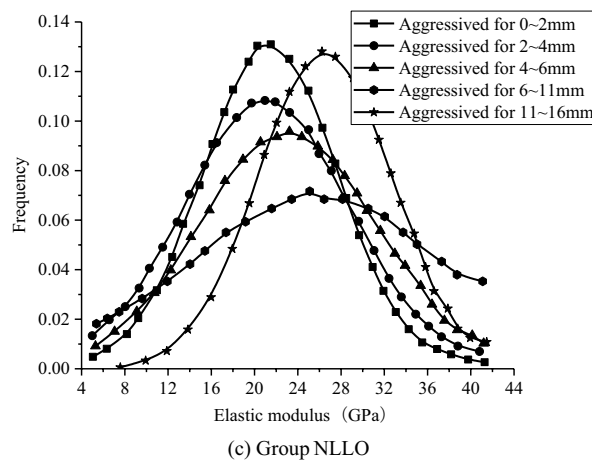
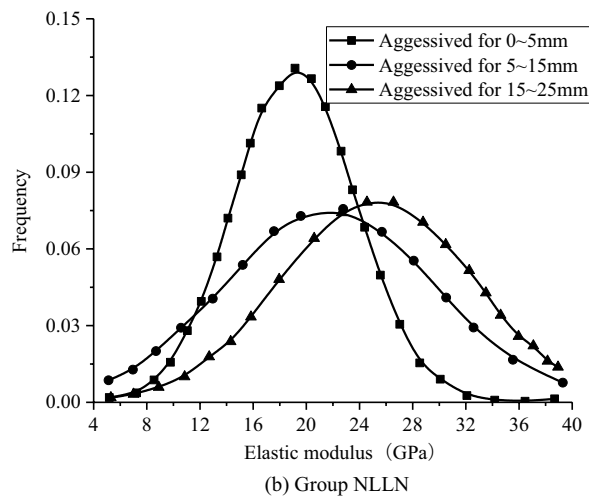
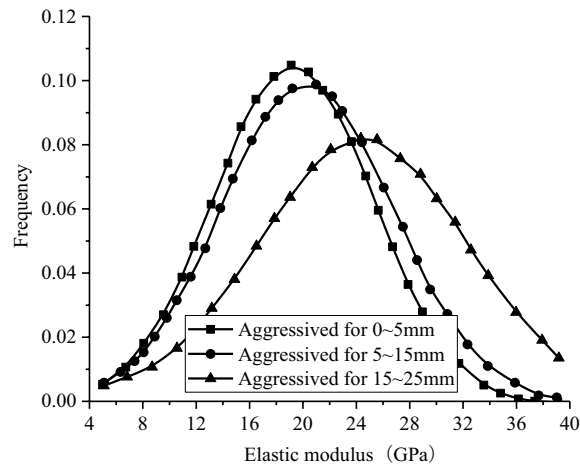


Figure 6. Probability fitting diagram of elastic moduli at different aggressive depths.

phase (from 0 to 45 days), the uniaxial compressive strength of group HLLN increased by 7.6%, whereas 31.5% and 17.3% increments took place in groups NSSN and NSCN, respectively. Hence, the uniaxial compressive strength growth of the samples in group B is significantly greater than that of in group HLLN. While in the slow decline stage (from 45 to 210 days), the uniaxial compressive strengths in groups HLLN, NSSN and NSCN showed gradual decrease trends. In addition, it is obvious that the uniaxial compressive strengths corresponding to group NSSN are highest, and the strengths corresponding to group HLLN are lowest in the above two stages. After being aggressed for 210 days, the uniaxial compressive strengths corresponding to group NSSN and

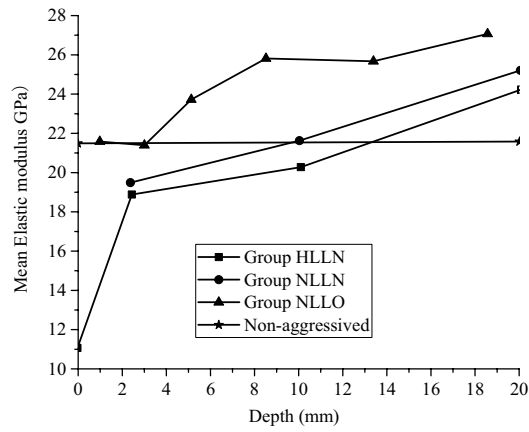


Figure 7. Elastic modulus at different aggressed depths.

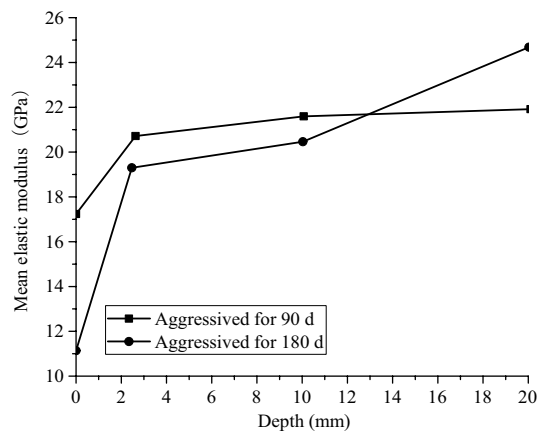


Figure 8. Modulus of elasticity at different aggressed depths for Group HLLN.

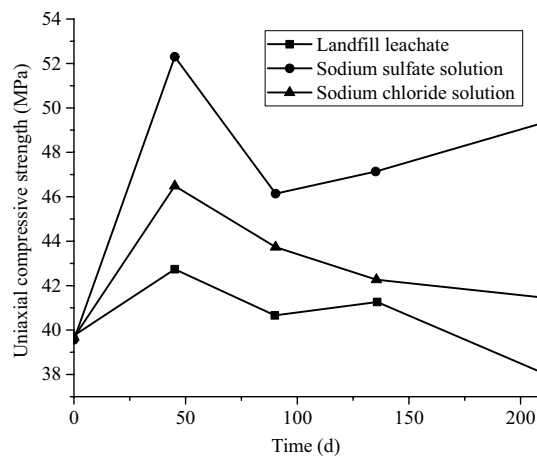


Figure 9. Uniaxial compressive strength of groups HLLN, NSSN, and NSCN after corrosion.

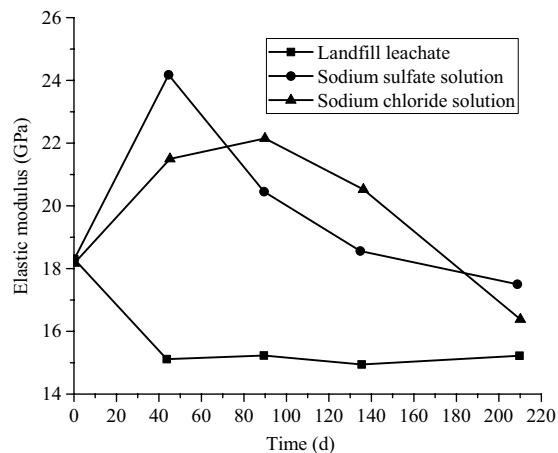


Figure 10. Elastic modulus of groups HLLN, NSSN, and NSCN after aggressiveness.

NSSN respectively increased by 20% and 5%, while the strength corresponding to group HLLN decreased by 5%. Therefore, it is concluded that compared with the sodium chloride and sodium sulfate solutions, the impact of landfill leachate on the strength of concrete and its macro-mechanical properties are the most significant in the short term.

According to Fig. 9, the uniaxial compressive strengths of the three conditions in the first stage show different increasing degrees, which attributes to the continuous hydration of concrete and secondary hydration effect of fly ash. In the linear increasing stage, because the components in landfill leachate of group HLLN weakened the above-mentioned effects, which eventually resulted in the lowest increase in the uniaxial compressive strength. While the compressive strength corresponding to group NSSN experienced a process of first decreasing and then increasing, which is due to the divalent sulfate ion reaction with the ions in the concrete, and the material produced by the reaction gradually hardened afterwards. After that, the compressive strength of group NSCN experienced a gradual decrease, the possible reason is that the aggressiveness effect of chloride ions on the concrete is gradually increased from the surface to inside. Therefore, the subsequent compressive strength change trend of group HLLN lies between group NSSN trend and group NSCN. In other words, it experienced a change from first decline, then a slight increase, and finally decline.

Deterioration law of elastic modulus. According to²⁶, the trends of elastic modulus for the three groups are shown in Fig. 10. It is obvious that the elastic moduli of the samples in landfill leachate decreased by 17.4% after being aggressived by group HLLN for 45 days, whose modulus changed from 18.274 to 15.092 GPa, and finally kept relatively stable. While the elastic modulus of the samples aggressived by group NSSN in the sodium sulfate solution increased by 32.2% corroded for 45 days, which finally reached 24.16 GPa and finally gradually decreased. Nevertheless, the elastic modulus of the group NSCN in the sodium chloride solution showed a relatively stable growth firstly and then gradually decreased. After being aggressived by the three solutions for 210 days, the elastic modulus of group HLLN, NSSN and NSCN decreased by 16.1%, 2.8% and 10.4%, respectively. Therefore, it is concluded that compared with the sodium sulfate and sodium chloride solutions, the change in the elastic modulus of concrete is more obvious after aggressived by the landfill leachate.

Conclusion

In order to study the evolution of the macro/micromechanical properties of the concrete aggressived by landfill leachate, this research focused on the behavior of the surfaces and different aggressived depths aggressived by high-concentration landfill leachate group HLLN, sodium sulfate solution group NSSN, sodium chloride solution group NSCN, landfill leachate original solution group NLLN and landfill leachate original solution plus osmotic pressure group NLLO. The main conclusions are as follows:

1. As the aggressiveness of the landfill leachate continues, a large number of microscopic cracks generated on the surface of the samples. At the same time, the hydration products with high elastic modulus such as C-S-H gel and calcium hydroxide in the concrete were consumed by the landfill leachate. The longer the aggressiveness of the high-concentration landfill leachate, the more severe the deterioration of the micromechanical properties of the sample surface.
2. The shallower the aggressived depth, the more severe the deterioration of the local meso-mechanical properties of the samples, the more severe the change in the mechanical properties, the less the content of hydration products with larger elastic modulus such as calcium hydroxide, and the more aggressive products with smaller elastic modulus such as pore and cracks.
3. The uniaxial compressive strength and elastic modulus of the concrete samples aggressived by landfill leachate showed a linear increase first and then slowly decrease with time. Compared with the sodium chloride and sodium sulfate solutions, the landfill leachate has the most significant weakening effect on the elastic modulus of concrete.

Received: 24 September 2021; Accepted: 15 February 2022

Published online: 10 March 2022

References

1. Wu, Q. Y., Ma, Q. Y. & Huang, X. W. Mechanical properties and damage evolution of concrete materials considering sulfate attack. *Materials* **14**, 23–43 (2021).
2. Islam, M. A., Golrokh, A. J. & Lu, Y. Chemo-mechanical modeling of sulfate attack-induced damage process in cement-stabilized pavements. *J. Eng. Mech.* **145**(1), 78–89 (2018).
3. Muthulingam, S. & Rao, B. N. Non-uniform corrosion states of rebar in concrete under chloride environment. *Corros. Sci.* **93**(apr.), 267–282 (2015).
4. Liu, S. W., Yang, Z. J. & Zhang, J. W. Mechanical properties of concrete under sustained sulfate soaking. *Bull. Chin. Ceram. Soc.* **39**(10), 3137–3142 (2020).
5. Lu, J. Z., Tian, L. Z., Liu, Y. & Tong, L. Q. Experimental study of the durability of concrete under coupling effect of axial compression and sulfate attack. *J. Basic Sci. Eng.* **28**(02), 386–395 (2020).
6. Fang, X. W., Lou, Z. K., Gao, Y. L. & Liu, P. Research progress on frost resistance durability of concrete under sulfate attack. *Concrete* **12**, 6–10+17 (2019).
7. Zafar, I. & Alqahtani, F. K. Effectiveness of extended curing for fly ash concrete against corrosion propagation under severe chloride exposure. *Struct. Concr.* **22**(5), 2688–2703 (2021).
8. Wu, L. J., Ju, X. L., Ma, Y. F. & Guan, L. Prediction model of chloride diffusion in concrete considering the blocking effects of rebar. *J. Build. Mater.* **24**(02), 296–303+332 (2021).
9. Li, B. Durability research on high strength ceramsite concrete at freezing–thawing cycles. *New Build. Mater.* **44**(08), 93–96 (2017).
10. Sun, X. H., Hu, D. L., Zhang, L. L., Chen, F. & Zha, B. Experimental study on carbonation of concrete components under freeze–thaw cycles and stress. *Bull. Chin. Ceram. Soc.* **39**(04), 1115–1125 (2020).
11. Du, J. M., Jiao, R. M., Han, X. L. & Ji, Y. S. Building of basic corrosion rate model of normal concrete based on corrosion thickness. *Concrete* **05**, 10–14 (2014).
12. Wang, L., Qin, H. G., Pang, C. M., et al. Durability of concrete under the corrosion of different salt. *Concrete*. **11**, 14–17 (2011).
13. Jiang, L. et al. Ultrasonic testing and microscopic analysis on concrete under sulfate attack and cyclic environment. *J. Centr. South Univ.* **21**, 4723–4731 (2014).
14. Zhao, Y. H. & Fan, Y. F. A theoretical model for assessing elastic modulus of concrete corroded by acid rain. *Eng. Mech.* **28**(2), 175–180 (2011).
15. Liu, H. K. & Li, J. Constitutive law of attacked concrete. *J. Build. Mater.* **14**(6), 736–741 (2011).
16. Hu, C., Gautam, B. P. & Panesar, D. K. Nano-mechanical properties of alkali-silica reaction (ASR) products in concrete measured by nano-indentation. *Constr. Build. Mater.* **158**, 75–83 (2018).
17. Fu, J. Nano-indentation experiment for determining mechanical properties of typical cement phases at nano/micro-scale. *IOP Conf. Ser. Mater. Sci. Eng.* **439**, 1–10 (2018).
18. Kjeldsen, P. et al. Present and long-term composition of MSW landfill leachate: A review. *CRC Crit. Rev. Environ. Control* **32**(4), 297–336 (2002).
19. Fleming, I. R. & Rowe, R. K. Laboratory studies of clogging of landfill leachate collection and drainage systems. *Can. Geotech. J.* **41**(4), 134–153 (2004).
20. Li, L. G. et al. Cementing efficiencies and synergistic roles of silica fume and nano-silica in sulphate and chloride resistance of concrete. *Constr. Build. Mater.* **223**, 965–975 (2019).
21. International Organization for Standards. *ISO 14577 Metallic Materials: Instrumented Indentation Test for Hardness and Materials Parameters-Part 1: Test Method* (International Organization for Standards, 2002).
22. Oliver, W. C. & Pharr, G. M. An improved technique for determining hardness and elastic modulus using load and displacement sensing indentation experiments. *J. Mater. Res.* **7**(6), 1564–1583 (1992).
23. Zhou, W. L., Sun, W., Chen, C. C. & Miao, C. W. Analysis of slag effect on micro-mechanical properties of cementitious materials by nanoindentation technique. *J. Chin. Ceram. Soc.* **39**(4), 718–725 (2011).
24. Qian, C., Nie, Y. & Cao, T. Sulphate attack-induced damage and micro-mechanical properties of concrete characterized by nano-indentation coupled with X-ray computed tomography. *Struct. Concr.* **17**(1), 96–104 (2016).
25. Haecker, C. J. et al. Modeling the linear elastic properties of Portland cement paste. *Cem. Concr. Res.* **35**(10), 1948–1960 (2005).
26. Sun, W. J. & Barlaz, M. A. Measurement of chemical leaching potential of sulfate from landfill disposed sulfate containing wastes. *Waste Manag.* **36**, 191–196 (2015).

Acknowledgements

The work presented in this paper is supported by the Natural Science Foundation of Shanxi under Grant Number 2020JM-626.

Author contributions

All work were done by W.F.

Competing interests

The author declares no competing interests.

Additional information

Correspondence and requests for materials should be addressed to W.F.

Reprints and permissions information is available at www.nature.com/reprints.

Publisher's note Springer Nature remains neutral with regard to jurisdictional claims in published maps and institutional affiliations.



Open Access This article is licensed under a Creative Commons Attribution 4.0 International License, which permits use, sharing, adaptation, distribution and reproduction in any medium or format, as long as you give appropriate credit to the original author(s) and the source, provide a link to the Creative Commons licence, and indicate if changes were made. The images or other third party material in this article are included in the article's Creative Commons licence, unless indicated otherwise in a credit line to the material. If material is not included in the article's Creative Commons licence and your intended use is not permitted by statutory regulation or exceeds the permitted use, you will need to obtain permission directly from the copyright holder. To view a copy of this licence, visit <http://creativecommons.org/licenses/by/4.0/>.

© The Author(s) 2022